Journal of NeuroVirology, 14: 5–16, 2008

ISSN: 1355-0284 print / 1538-2443 online
DOI: 10.1080/13550280701750635

informa
healthcare

Chemokine expression during mouse hepatitis virus-induced encephalitis: Contributions of the spike and background genes

Erin P Scott,[1] Patrick J Branigan,[2] Alfred M Del Vecchio,[2] and Susan R Weiss[1]

[1]*Department of Microbiology, University of Pennsylvania, School of Medicine, Philadelphia, Pennsylvania, USA*
[2]*Centocor Inc., Radnor, Pennsylvania, USA*

Infection of mice with mouse hepatitis virus (MHV) strain JHM (RJHM) induces lethal encephalitis, with high macrophage and neutrophil, but minimal T-cell, infiltration into the brain when compared to the neuroattenuated strain RA59. To determine if chemokine expression corresponds with the cellular infiltrate, chemokine protein and RNA levels from the brains of infected mice were quantified. RJHM-infected mice had lower T-cell (CXCL9, CXCL10), but higher macrophage-attracting (CCL2), chemokine proteins compared to RA59. RJHM also induced significantly higher CXCL2 (a neutrophil chemoattractant) mRNA compared to RA59. The neurovirulent spike gene chimera SJHM/RA59 induces high levels of T cells and macrophages in the brain compared to the attenuated SA59/RJHM chimera. Accordingly, SJHM/RA59 induced higher levels of CXCL9, CXCL10, and CCL2 protein compared to SA59/RJHM. Chemokine mRNA patterns were in general agreement. Thus, chemokine patterns correspond with the cellular infiltrate, and the spike protein influences levels of macrophage, but not T-cell, chemokines. *Journal of NeuroVirology* (2008) **14,** 5–16.

Keywords: cytokines; MHV; macrophage; neutrophil; T cell

Introduction

Viral encephalitis is of notable health concern in the United States and worldwide. For instance, there have been over 9500 reported cases of West Nile–associated encephalitis or meningitis in the United States since 1999 (Centers for Disease Control, 2006). Over 1700 people died of Japanese encephalitis during a large outbreak in India and Nepal in 2005 (World Health Organization, 2005). The manifestations of viral encephalitides vary widely in the human population, from mild, flulike symptoms to severe encephalitis. Therefore, a comparative model of viral encephalitis is ideal for determining host and viral factors that contribute to the variation in severity. We utilize two strains of the coronavirus mouse hepatitis virus (MHV) to provide such a model. In mice, strain JHM (MHV-4 isolate) has a lethal dose (LD_{50}) of approximately one plaque forming unit (PFU) following intracranial (i.c.) inoculation, with death resulting from severe encephalitis within one week (Dalziel *et al*, 1986; Phillips *et al*, 1999). In contrast, strain A59 has an LD_{50} of 3000 PFU, and i.c. inoculation results in mild encephalitis and moderate hepatitis, with mice recovering from acute disease within 2 weeks (Lavi *et al*, 1984b).

Cell-mediated immunity is clearly important to the outcome of infection. It has been demonstrated that both CD4+ and CD8+ T cells are critical for clearance of MHV from the brain (Lane *et al*, 2000; MacNamara *et al*, 2005; Williamson and Stohlman, 1990). The production of interferon (IFN)-γ also correlates with viral clearance (Lane *et al*, 1997; Parra *et al*, 1997; Pearce *et al*, 1994; Rempel *et al*, 2004a;

Address correspondence to Susan Weiss, Department of Microbiology, University of Pennsylvania, 3610 Hamilton Walk, Philadelphia, PA 19104-6076, USA. E-mail: weisssr@mail.med.upenn.edu

This work was supported by NIH grant A1-60021. E.P.S. was supported by training grant NS07180. The authors would like to thank Jessica Roth-Cross and Susan Roth for help collecting the brains.

Received 28 June 2007; revised 15 August 2007; accepted 12 September 2007.

Smith *et al*, 1991). Accordingly, a robust T-cell and IFN-γ response is induced in the brain during A59 infection, resulting in the clearance of infectious virus, although viral RNA persists in the central nervous system (Iacono *et al*, 2006; Lavi *et al*, 1984a; Rempel *et al*, 2004a). Conversely, JHM infection induces a poor T-cell response and low levels of IFN-γRNA, but a robust macrophage and neutrophil infiltration (Iacono *et al*, 2006; Rempel *et al*, 2004a).

Viral genetic factors have also been implicated in the outcome of disease. The spike glycoprotein (S) of MHV is responsible for receptor binding and virus-cell fusion during entry (Collins *et al*, 1982). To investigate the contribution of S to MHV pathogenesis, we have previously constructed recombinant chimeric viruses in which the S gene of A59 was replaced with the S of JHM and vice versa (SJHM/RA59, SA59/RJHM) (Navas and Weiss, 2003; Phillips *et al*, 1999). Wild-type recombinants RJHM and RA59 were also constructed and were phenotypically indistinguishable from parental viruses JHM (also called MHV-4 or JHM_{SD}) (Navas *et al*, 2001) and A59 (Phillips *et al*, 1999). Infection with SJHM/RA59 resulted in increased mortality, inflammation, and viral antigen spread when compared to RA59 (Phillips *et al*, 1999, 2002). Interestingly, the T-cell response to the SJHM/RA59 remained robust, and was in fact greater than that induced by RA59 (Iacono *et al*, 2006; Phillips *et al*, 2002; Rempel *et al*, 2004a). The reciprocal recombinant virus SA59/RJHM was neuroattenuated, resulting in low mortality and greatly reduced antigen spread and inflammation when compared to RJHM (Iacono *et al*, 2006). The T-cell response to SA59/RJHM was also low, with total virus-specific CD8+ T-cell numbers in the brain similar to those observed during RJHM infection (Iacono *et al*, 2006). In contrast to the T-cell infiltration, RJHM and SJHM/RA59 both induced elevated levels of macrophages when compared to RA59 and SA59/RJHM (Iacono *et al*, 2006). Elevated neutrophil infiltration was only observed following RJHM infection when compared to other strains (Iacono *et al*, 2006). Together, these results indicate that neurovirulence and macrophage infiltration is at least partially mediated by the S gene, whereas T-cell infiltration is mediated by proteins other than spike. Neutrophil infiltration, however, is not solely dependent on either S or background genes, but is characteristic of RJHM alone.

The reasons for the observed differential pattern of cellular infiltration in response to RA59 and RJHM are unclear. One contributing factor may be that RJHM and RA59 induce differential chemokine patterns, resulting in the recruitment of different cell populations. Chemokines are a group of proteins that recruit and activate immune cells in response to infection or injury. Chemokine levels are often altered during viral encephalitis and their upregulation correlates with the influx of cellular infiltrates (Asensio and Campbell, 2001). Chemokines such as CXCL9 (MIG, monokine induced by IFN-γ) and CXCL10 (IP-10, IFN-inducible protein-10) have been demonstrated to attract activated T cells and can be produced in the brain in response to viral infection (Asensio *et al*, 2001; Klein *et al*, 2005; Marques *et al*, 2006; Patterson *et al*, 2003; Ransohoff *et al*, 2002; Sellner *et al*, 2005; Xu *et al*, 2005). Other chemokines, such as CCL2 (MCP-1, monocyte chemoattractant protein), CCL7 (MCP-3), CCL3 (MIP-1α, macrophage inflammatory protein), and CCL4 (MIP-1β) attract macrophages, although these chemokines attract T cells as well (Loetscher *et al*, 1994; Matsushima *et al*, 1989; Standiford *et al*, 1993; Wang *et al*, 1993). Murine neutrophil chemoattractants include CXCL2 (MIP-2) and Keratinocyte-derived cytokine (KC) Bozic *et al*, 1995; Wolpe *et al*, 1989). Many of these chemokines have been reported to be produced in neural cell types, including astrocytes, microglia, and neurons, in response to viral infection (Klein *et al*, 2005; Lane *et al*, 1998; Marques *et al*, 2006; Patterson *et al*, 2003; Rubio *et al*, 2006). It is possible that infected cells may produce different chemokine patterns in response to the two virus strains. Indeed, it has previously been demonstrated that CCL3, CCL4, and CXCL2 mRNAs were elevated in the brains of MHV-4–infected mice when compared to RA59-infected mice (Rempel *et al*, 2004a). The expression kinetics of T cell– and other macrophage-attracting chemokines has not been previously demonstrated in a comparative model of MHV.

In order to determine if RJHM and RA59 infection induce differential patterns of chemokines in the brain that could influence cellular infiltration, we quantified T cell–, macrophage-, and neutrophil-attracting chemokines, at both the protein and mRNA levels, during the course of infection. Our results indicate that T cell–attracting chemokine levels in the brain correspond to the differential CD8+ T-cell responses characteristic of the MHV strains used in this study. Macrophage- and neutrophil-attracting chemokine levels also correlate with patterns of macrophage and neutrophil infiltrates, particularly late in infection. In addition, by the use of chimeric recombinant viruses in which the S genes have been exchanged, we demonstrate that T cell–attracting chemokines appear to be influenced by genes other than S, whereas macrophage-attracting chemokines appear to be influenced by the S gene.

Results

Levels of MHV genomic RNA in the brain over the course of infection

Viral genomic RNA was measured by real-time reverse transcriptase–polymerase chain reaction (RT–PCR) to compare the levels of viral genomes present in the brain after infection with RJHM, RA59, SJHM/RA59, or SA59/RJHM, and to confirm

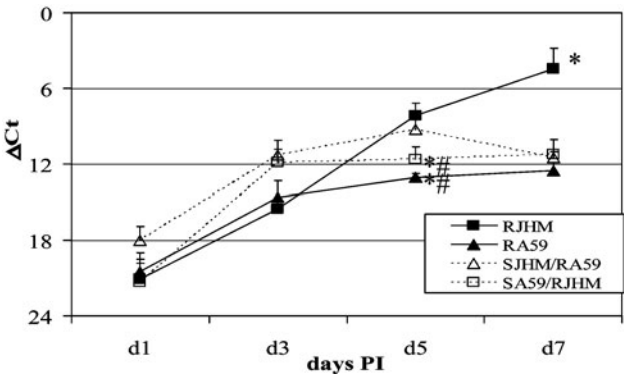

Figure 1 MHV genome levels in the brain throughout infection. Mice were inoculated i.c. with RJHM, RA59, SJHM/RA59, or SA59/RJHM and sacrificed at the indicated time points. RNA was isolated from the brain and analyzed by real-time RT–PCR for MHV genome expression. Data represent average ΔCt values ($\Delta Ct = Ct_{genome} - Ct_{18S}$) per group combined from two independent experiments + SEM. $^{*}P < .01$ versus RA59; $^{\#}P < .05$ versus SA59/RJHM. (d1 $n = 7$–9; d3 $n = 3$–10; d5 $n = 6$–10; d7 $n = 2$–10.)

infection of mice (Figure 1). At day 5 post infection (p.i.), RJHM genomes in the brain were significantly higher than SA59/RJHM and RA59 (12- and 32-fold, respectively). SJHM/RA59 genomes were also significantly higher than SA59/RJHM and RA59 (5- and 16-fold, respectively). At day 7 p.i., whereas the number of SJHM/RA59 genomes dropped, RJHM genome levels continued to increase and were as much as 250-fold higher than the other three viruses (Figure 1). This is consistent with the difference in neurovirulence among the viruses. While the host is unable to control RJHM infection, genome RNA levels continue to increase at day 7 at a time which the majority of RJHM-infected animals have died from encephalitis; animals infected with the other viruses clear infection, consistent with the leveling off of genome RNA levels at day 7.

T-cell chemokine protein and mRNA levels in MHV-infected brains

We utilize two different strains of MHV that result in a poor (RJHM) or robust (RA59) T-cell infiltration. We therefore wanted to determine if there are differences in the levels of CXCL9 and/or CXCL10 in the brain during infection with RJHM and RA59 that may explain the disparity in T-cell infiltration. Mice were inoculated intracranially (i.c.) with 50 plaque-forming units (PFU) of the recombinant viruses RJHM, RA59, or mock-infected. At days 3 and 5 p.i., brains were collected and half of the brain homogenized in phosphate-buffered saline (PBS) to quantify protein levels via bead-based protein multiplex technology (Luminex). From the same animals, we also measured cytokine mRNA to confirm protein data and to detect the expression of chemokines that were either untested or undetectable at the protein level. Chemokine mRNA levels were determined at days 1, 3, 5, and 7 p.i. using low-density array (LDA) cards.

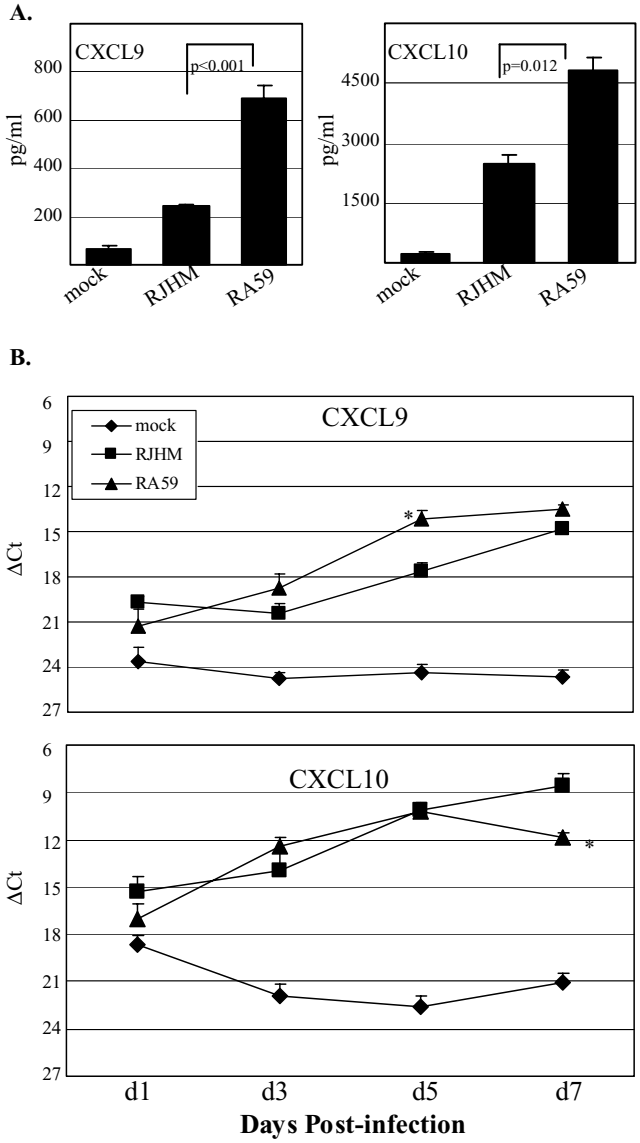

Figure 2 CXCL9 and CXCL10 expression in the brain following RJHM and RA59 infection. RNA and protein was isolated from the brains of infected mice and analyzed by real-time RT-PCR for mRNA levels using LDA cards or protein expression by a bead array assay as described in Materials and Methods. (**A**) Chemokine protein expression at day 5 post infection ($n = 2$–5). Bars represent averages per group + SEM. (**B**) Kinetics of chemokine mRNA expression. Data represent average ΔCt values ($\Delta Ct = Ct_{cytokine} - Ct_{18S}$) per group combined from two independent experiments + SEM. $^{*}P < .01$ versus RJHM. (d1 $n = 9$–10; d3 $n = 9$–10; d5 $n = 6$–10; d7 $n = 2$–10.)

At day 5 p.i., the protein levels of the T-cell chemoattractants CXCL9 (MIG) and CXCL10 (IP-10) were significantly higher in RA59-infected brains when compared to RJHM-infected brains (Figure 2A). There were no differences between virus groups in protein levels observed at day 3, although CXCL9 was significantly higher in infected brains compared to mock (data not shown). Comparison of mRNA revealed that similar to the results on protein levels,

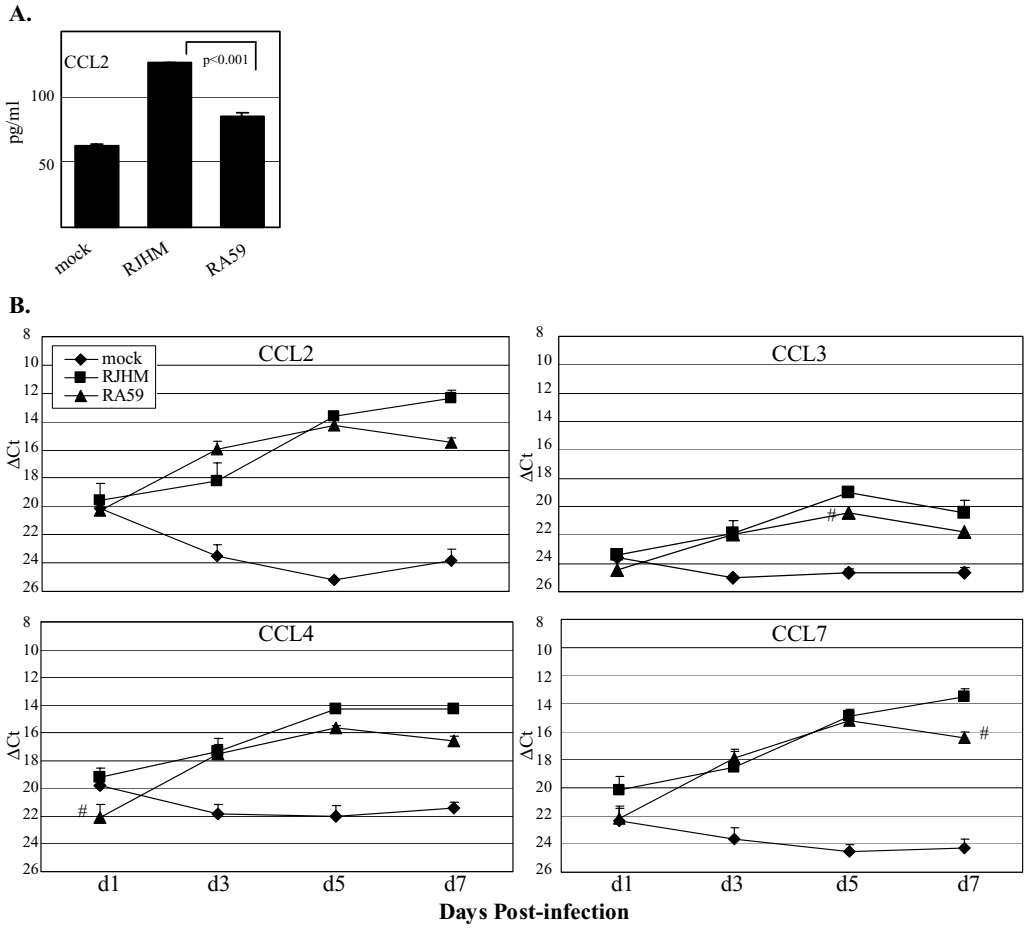

Figure 3 Macrophage chemokine expression in the brain after RJHM and RA59 infection. RNA and protein was isolated from the brains of infected mice and analyzed by real-time RT–PCR for mRNA levels using LDA cards or protein expression by a bead array assay as described in Materials and Methods. (**A**) Chemokine protein expression at day 5 post infection ($n = 2$–5). Bars represent averages per group + SEM. (**B**) Kinetics of chemokine mRNA expression. Data represent average ΔCt values ($\Delta Ct = Ct_{cytokine} - Ct_{18S}$) per group combined from two independent experiments + SEM. $^{\#}P < .05$ versus RJHM. (d1 $n = 9$–10; d3 $n = 3$–10; d5 $n = 7$–10; d7 $n = 2$–10.)

CXCL9 mRNA in the brain was 10-fold higher in RA59-infected mice compared to RJHM at day 5 (Figure 2B). However, unlike the protein results, there were no differences for CXCL10 mRNA at day 5, and in fact, RA59-infected brains had 9-fold lower levels than RJHM at day 7 (Figure 2B). These data suggest that differential CXCL9 and CXCL10 expression in the brain contributes to the differential T-cell infiltrate observed between RJHM and RA59 infection.

Macrophage chemokine protein and mRNA levels in MHV-infected brains

Macrophage infiltration into the brain is much higher following RJHM infection than RA59 infection (Iacono *et al*, 2006; Rempel *et al*, 2004a). To determine if macrophage-attracting chemokine levels also corresponded with the kinetics and levels of macrophage infiltration, protein and mRNA levels of several known macrophage chemokines were measured. Protein levels of CCL2 (MCP-1) were significantly higher in RJHM-infected brains compared to RA59-infected brains at day 5 p.i. (Figure 3A). However, CCL2 mRNA levels were not significantly different (Figure 3B). Although protein was not detectable for CCL3 (MIP-1α; Data not shown), mRNA levels were 2.5-fold higher in RJHM-infected brains compared to RA59 at day 5 (Figure 3B). The mRNA levels of CCL4 (MIP-1β) were 9-fold higher in RJHM-infected brains at day 1, whereas CCL7 (MCP-3) mRNA was approximately 8-fold higher for RJHM-infected animals than RA59 infected mice at day 7 (Figure 3B). At day 3 p.i., although CCL2 protein levels were elevated above mock in both RJHM- and RA59-infected brains, there were no significant differences between RJHM- and RA59-infected brains for any of the chemokines at either the protein or mRNA level (data not shown; Figure 3B). Although the differences are not very large, it appears that macrophage chemokines are generally higher in the brains of RJHM infected mice, which corresponds to the higher levels of macrophages present.

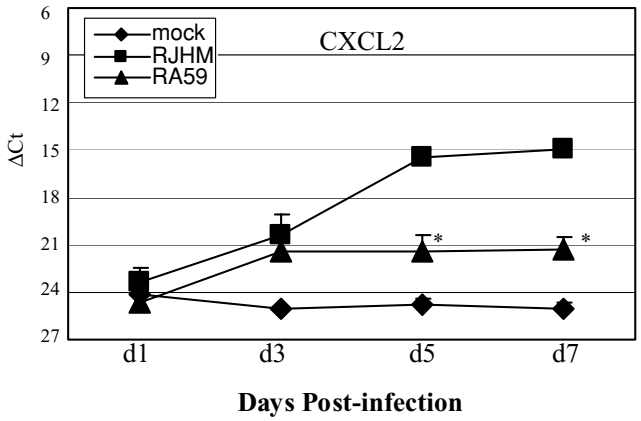

Figure 4 CXCL2 mRNA expression in the brain after RJHM and RA59 infection. RNA was isolated from the brains of infected mice and analyzed by LDA cards for mRNA levels as described in Materials and Methods. Data represent average ΔCt values ($\Delta Ct = Ct_{cytokine} - Ct_{18S}$) per group combined from two independent experiments + SEM. $^{*}P < .01$ versus RJHM. (d1 $n = 9$–10; d3 $n = 9$–10; d5 $n = 6$–10; d7 $n = 2$–10.)

Neutrophil chemokine mRNA expression in MHV-infected brains

Large numbers of neutrophils are also observed in the brains of RJHM-infected mice, with peak infiltration occurring at day 7 (Iacono *et al*, 2006). Both RJHM- and RA59-infected brains had significantly higher levels of CXCL2 (MIP-2), a neutrophil-attracting chemokine, compared to mock-infected brains at days 5 and 7 p.i. However, levels of CXCL2 were much higher (64-fold) in RJHM-infected brains at both days 5 and 7 compared to RA59 (Figure 4). Although CXCL2 was not measured on the protein level, these data indicate that, at least on the mRNA level, CXCL2 is elevated during RJHM infection of the brain, corresponding to the high levels of neutrophil infiltration.

T-cell chemokine protein and mRNA expression are influenced by genes other than spike

Using recombinant viruses in which the S gene has been exchanged between RJHM and RA59, we have previously demonstrated that the spike (S) gene is a major determinate of neurovirulence. (Iacono *et al*, 2006; Phillips *et al*, 1999, 2002). Importantly, SJHM/RA59 induces a stronger T-cell response than either RJHM or RA59, whereas SA59/RJHM, like RJHM, induces a minimal CD8+ T-cell response in the brain (Iacono *et al*, 2006; Phillips *et al*, 2002; Rempel *et al*, 2004b). These data suggest that the infiltration of T cells is not influenced by the S gene. To determine if viral genes other than S influence T-cell chemokine responses, in the same experiments described for RJHM and RA59 above, mice were also infected with SJHM/RA59 and SA59/RJHM and chemokine mRNA and protein levels were also quantified from their brains.

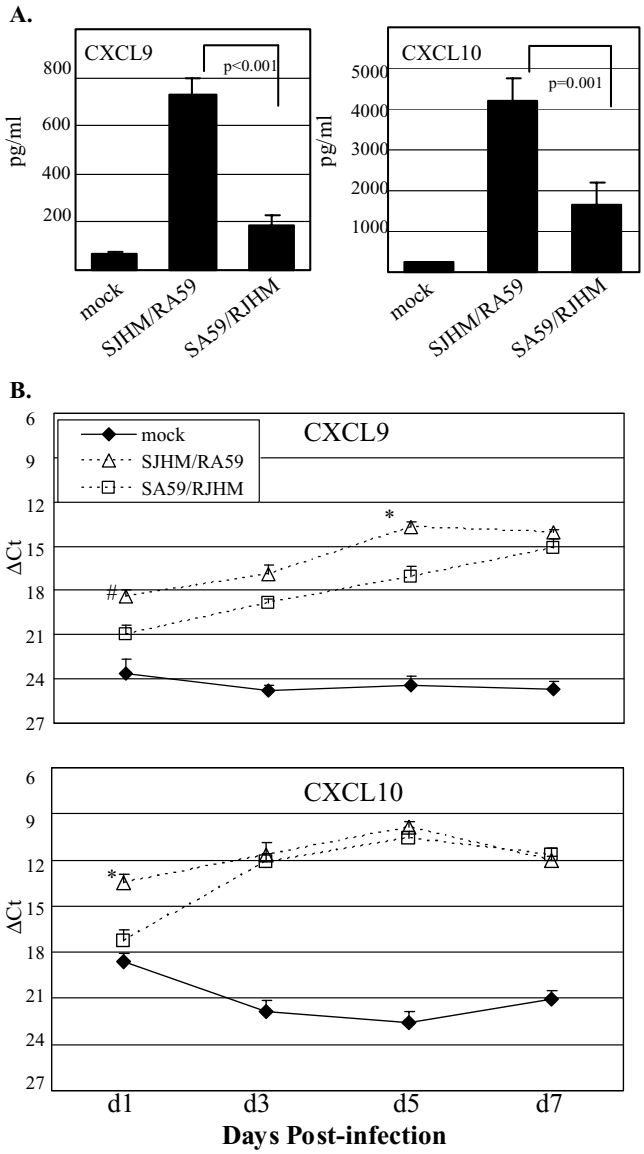

Figure 5 CXCL9 and CXCL10 expression in the brain after SJHM/RA59 and SA59/RJHM infection. RNA and protein was isolated from the brains of infected mice and analyzed by real-time RT-PCR for mRNA levels using LDA cards or protein expression by a bead array assay as described in Materials and Methods. (**A**) Chemokine protein expression at day 5 post infection ($n = 5$). Bars represent averages per group + SEM. (**B**) Kinetics of chemokine mRNA levels. Data represent average ΔCt values ($\Delta Ct = Ct_{cytokine} - Ct_{18S}$) per group combined from two independent experiments + SEM. $^{\#}P < .05$, $^{*}P < .01$ versus SA59/RJHM. (d1 $n = 10$; d3 $n = 3$–10; d5 $n = 7$–10; d7 $n = 6$–10.)

At the protein level, CXCL9 and CXCL10 were both significantly higher in SJHM/RA59-infected brains than SA59/RJHM at day 5 (Figure 5A). In agreement with protein levels, CXCL9 and CXCL10 mRNA levels were both significantly higher in SJHM/RA59-infected brains compared to SA59/RJHM at day 1 (Figure 5B). CXCL9 mRNA remained significantly higher at day 5 in the SJHM/RA59-infected brains compared to SA59/RJHM-infected brains (Figure 5B).

Therefore, in comparison to the wild-type viruses, T cell–attracting chemokine expression from SJHM/RA59-infected brains is similar to RA59, and SA59/RJHM is similar to RJHM. These results indicate that T-cell chemoattractants appear to be influenced by genes other than the S gene.

The S gene influences macrophage chemokine protein and mRNA expression

Using the isogenic recombinant viruses SJHM/RA59 and SA59/RJHM, we have previously demonstrated that, in contrast to T-cell infiltration, macrophage infiltration into the brain is influenced by the S gene (Iacono *et al*, 2006). We analyzed the expression of macrophage chemoattractants in the brain during SJHM/RA59 and SA59/RJHM infection to determine if they were also influenced by the S gene. At the protein level, CCL2 was significantly higher in SJHM/RA59-infected brains compared to SA59/RJHM at day 5 (Figure 6A). CCL3 protein levels were not detectable (data not shown). The mRNA results for CCL2 also showed elevated levels in SJHM/RA59-infected brains compared to SA59/RJHM at both days 1 and 5 p.i. (Figure 6B). CCL7 mRNA was also elevated in SJHM/RA59-infected brains compared to SA59/RJHM at day 1 only (Figure 6B). There were no differences at any timepoint in the mRNA levels of CCL3 or CCL4 (data not shown). These data, in combination with the results shown for wild-type recombinant viruses in Figure 3, demonstrate that macrophage chemokine patterns, particularly CCL2, are influenced by the S gene.

IFN-γ and IL-12 cytokine protein and mRNA levels are influenced by genes other than spike

CXCL9 and CXCL10 are both induced by IFN-γ (Farber, 1990; Luster and Ravetch, 1987) and IFN-γ is induced by IL-12. The presence of these two cytokines is usually considered a hallmark of a Th1 T-cell response. It has been reported previously that RJHM infection does not induce as much IFN-γ or IL-12 mRNA as RA59, which may explain the lower levels of CXCL9 and CXCL10 in the brain during RJHM infection. (Rempel *et al*, 2004a). We wanted to extend these results with a quantitative assay and analyze the kinetics of IFN-γ and IL-12 expression in parallel with T cell–attracting chemokine expression. Using the same protein and mRNA samples as described above, we found that although there was a trend toward higher IFN-γ and IL-12 protein in RA59 infected brains at day 5 p.i., this difference did not reach statistical significance (P =. 094 and. 095 respectively) (Figure 7A). However, at the mRNA level, IFN-γ expression was significantly higher during RA59 infection at days 3 and 5 p.i. when compared to RJHM infection (Figure 7B). There were no differences for IL-12p40 mRNA between RA59- and RJHM-infected brains (data not shown). Notably, there were no differences between groups detected at either the protein or mRNA level for the Th2 cytokines interleukin (IL)-4, IL-5, or IL-10 (data not shown).

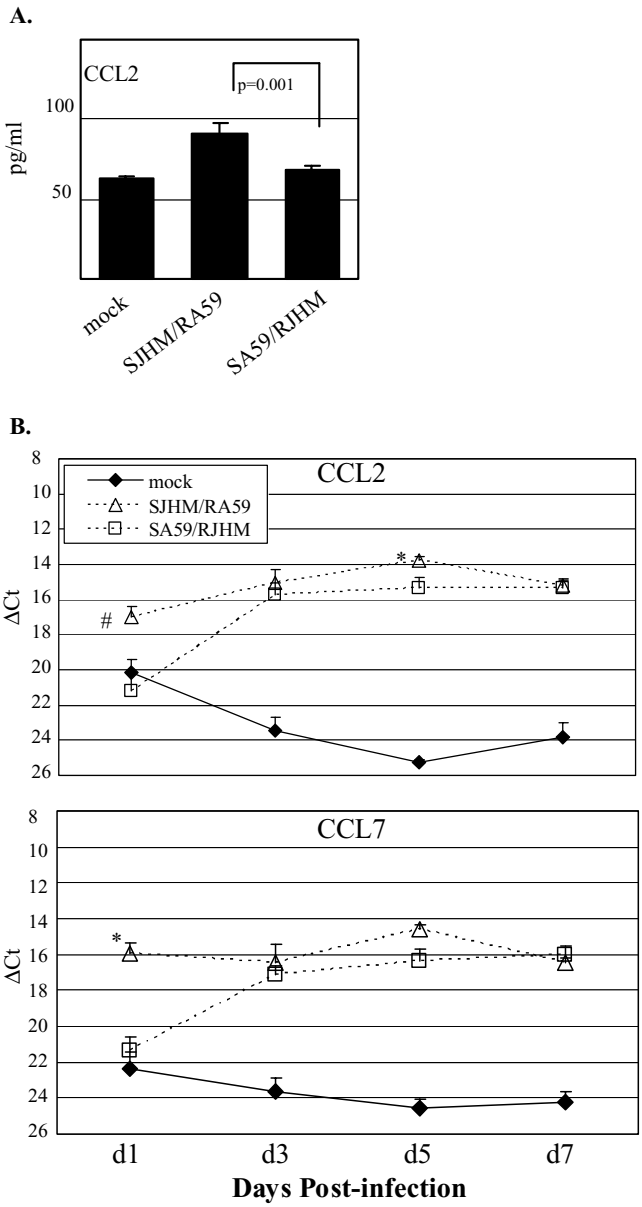

Figure 6 CCL2 and CCL7 expression in the brain after SJHM/RA59 and SA59/RJHM infection. RNA and protein were isolated from the brains of infected mice and analyzed by real-time RT-PCR for mRNA levels using LDA cards or protein expression by a bead array assay as described in Materials and Methods. (**A**) Chemokine protein expression at day 5 post infection ($n = 5$). Bars represent averages per group + SEM. (**B**) Kinetics of chemokine mRNA levels. Data represent average ΔCt values ($\Delta Ct = Ct_{cytokine} - Ct_{18S}$) per group combined from two independent experiments + SEM. $^{\#}P < .05$, $^{*}P < .01$ versus SA59/RJHM. (d1 $n = 10$; d3 $n = 3$–10; d5 $n = 7$–10; d7 $n = 6$–10.)

Our data indicated that genes other than S influence expression of T cell–attracting chemokines during MHV infection of the brain. We hypothesized that cytokines that influence these chemokines, IFN-γ and IL-12, would also be under the control of genes other than S. Protein levels of IFN-γ and IL-12 in the brain were significantly higher after SJHM/

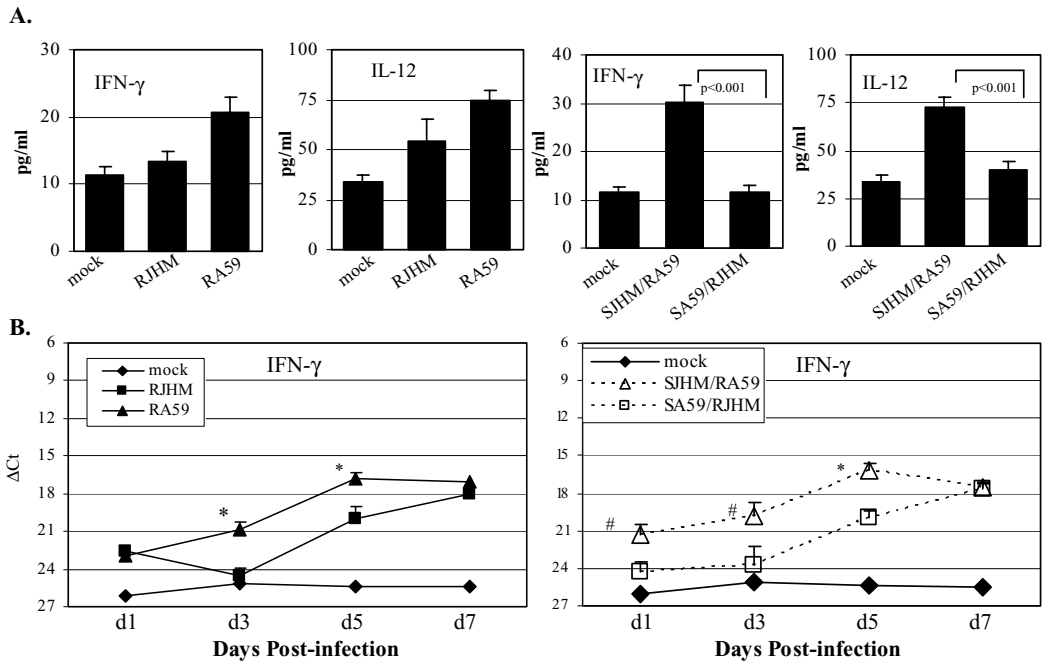

Figure 7 IFN-γ and IL-12 expression in the brain after RJHM, RA59, SJHM/RA59, and SA59/RJHM infection. RNA and protein were isolated from the brains of infected mice and analyzed by real-time RT–PCR for mRNA levels using LDA cards or protein expression by a bead array assay as described in Materials and Methods. (**A**) Chemokine protein expression at day 5 post infection ($n = 5$). Bars represent averages per group + SEM. (**B**) Kinetics of chemokine mRNA levels. Data represent average ΔCt values ($\Delta Ct = Ct_{cytokine} - Ct_{18S}$) per group combined from two independent experiments + SEM. $^*P < .01$ versus RJHM. (d1 $n = 9$–10; d3 $n = 3$–10; d5 $n = 6$–10; d7 $n = 2$–10.)

RA59 infection when compared to SA59/RJHM at day 5 (Figure 7A). Although there were no significant differences between groups for IL-12p40 mRNA, mRNA levels for IFN-γ were significantly higher in SJHM/RA59-infected brains compared to SA59/RJHM at days 1, 3, and 5 p.i. (Figure 7B). The data for IFN-γ and IL-12 indicate their pattern of expression parallels CXCL9 and CXCL10 expression. All four cytokines appear to correspond with the patterns of T-cell infiltration, and all four also appear to be under the influence of background genes other than S.

In summary, chemokine patterns parallel the cellular infiltration observed during infection with different strains of MHV (Table 1). Macrophage-attracting chemokine expression is influenced by the spike protein, whereas T cell–attracting chemokines and Th1 cytokines are influenced by background genes. Very high expression of neutrophil-attracting chemokine mRNA occurs only in response to the RJHM alone.

Discussion

The elevation of chemokine levels has been documented in several models of viral encephalitis. (Manchester *et al*, 1999; Sanders *et al*, 1998; Shirato *et al*, 2004; Winter *et al*, 2004), including MHV (Lane *et al*, 1998; Rempel *et al*, 2004a). In previous studies with MHV, i.c. infection with V5A13.1 (a neuroattenuated variant of JHM that does induce T-cell infiltration [Liu *et al*, 2001, 2000]) resulted in elevated mRNA levels of CXCL9, CXCL10, CCL5, CCL2,

Table 1 Summary of cellular infiltrate and chemokine pattern in the brain with MHV virus

	Cellular infiltrate[a]			*Chemokine pattern*[b]		
Virus	*T-cell*	*Macrophage*	*Neutrophil*	*T-cell*	*Macrophage*	*Neutrophil*
RJHM	+	+++	+++	+	++	+++
RA59	++	+	+/−	+++	+/−	+
SJHM/RA59	+++	++	+/−	+++	+	+
SA59/RJHM	+/−	+/−	+/−	+	−	+

[a]Estimates of total number of cells per brain adapted from Iacono *et al* (2006) day 7 post infection.
[b]Estimates for day 5 post infection. T-cell chemokine levels are representative of CXCL9 and CXCL10 protein. Macrophages chemokine levels are representative of CCL2 protein and CCL2, CCL3, CCL7 mRNA. Neutrophil chemokine levels are representative of CXCL2 mRNA.

CCL4, CCL7, and CXCL2 in the brain when compared to mock-infected brains (Lane *et al*, 1998; Liu *et al*, 2001; Stiles *et al*, 2006b). T cell–attracting chemokine responses in a comparative MHV model (RJHM versus RA59) were characterized to determine if the chemokine patterns could explain their differential T-cell responses. Protein levels for both CXCL9 and CXCL10, as well as the mRNA for CXCL9, are elevated during RA59 infection compared to RJHM at day 5 p.i. This observation corresponds with the kinetics of T-cell infiltration, which is detected by day 5, but peaks at day 7, p.i. (Iacono *et al*, 2006; Phillips *et al*, 2002). CXCL9 and CXCL10 have previously been demonstrated to be important for T-cell infiltration during infection with JHM variant V5A13.1, in that infection of both CXCL9/10$^{-/-}$ mice, or treatment with anti-CXCL9/10 antibodies, decreased T-cell infiltration and increased viral replication and mortality (Dufour *et al*, 2002; Glass *et al*, 2002; Liu *et al*, 2001; Liu *et al*, 2000). Interestingly, following infection of CXCL10$^{-/-}$ mice with JHM-DM (another strain which induces a T-cell response) virus-specific T cells were still generated and could proliferate, although IFN-γ–producing CD8+ T-cell numbers were reduced (Stiles *et al*, 2006a). There was also no defect in expression of the CXCL10 receptor (CXCR3) or effector functions such as CTL activity (Stiles *et al*, 2006a). Together, these data indicate that CXCL10 is important for T-cell chemoattraction but not T-cell generation or function during MHV infection.

Aside from chemokine expression, there may be other explanations for the differential T-cell responses during RJHM and RA59 infection. Using an adoptive transfer model, we have demonstrated that CD8+ T cells are not being effectively primed during RJHM infection (MacNamara *et al*., submitted for publication). Because CXCL9 and CXCL10 are chemoattractants for activated T cells, as opposed to naïve T cells (Farber, 1997), even if RJHM induced these chemokines, there would only be a small amount of activated T cells for these chemokines to attract. Thus, there appear to be multiple levels at which RJHM infections compromises the infiltration of T cells into the brain.

Another major difference between RJHM and RA59 infection is the high level of macrophages observed in the brain during RJHM infection starting by day 5 p.i., and peaking at day 7 (Iacono *et al*, 2006; Rempel *et al*, 2004a). We hypothesized macrophage chemoattractant levels would parallel macrophage infiltration. CCL2, CCL3, CCL4, and CCL7 are macrophage-attracting chemokines, although it should be noted that these cytokines are also chemoattractants for T cells (Loetscher *et al*, 1994). Protein levels at day 5 p.i. indicate that RJHM-infected brains have higher levels of CCL2 than RA59. Higher levels of mRNA for other macrophage-attracting chemokines were observed in RJHM-infected brains. Most studies investigating macrophage involvement during MHV infection have been focused on the demyelination that occurs after recovery from encephalitis (reviewed in. Glass *et al*, 2002). However, the potential damage to neurons by infiltrating macrophages during the acute phase should not be ignored. The overexpression of the chemokines themselves may have adverse effects on neurons. CCL2, for example, has been demonstrated to decrease Purkinje neuron excitability and alter intracellular Ca^{2+} levels (van Gassen *et al*, 2005).

The S gene has been demonstrated to be a determinant of neurovirulence and to influence macrophage, but not T-cell infiltration (Iacono *et al*, 2006; Phillips *et al*, 1999, 2002; Rempel *et al*, 2004b). We also wanted to determine whether the S or background genes would influence T cell–, macrophage-, or neutrophil-attracting chemokine expression. The chimeric SJHM/RA59, which induces a robust T-cell response, also induces higher CXCL9 and CXCL10 expression compared to SA59/RJHM, indicating that like the T-cell response itself, the expression of T-cell chemokines during MHV infection is influenced by genes other than S. In contrast, macrophage infiltration is also high during SJHM/RA59 infection, but not during SA59/RJHM infection, suggesting that macrophage infiltration is influenced by the S gene (Iacono *et al*, 2006). Accordingly, our analysis of the macrophage chemokine response (Figures 3, 6) demonstrates an association between the JHM S gene and elevated expression of macrophage chemoattractants. In support of this conclusion, previous studies reported higher mRNA levels of CCL3 and CCL4 in the brain following both RJHM and SJHM/RA59 infection compared to RA59 (Rempel *et al*, 2004b).

The influx of neutrophils during RJHM infection peaks at day 7, whereas RA59, SJHM/RA59, and SA59/RJHM do not induce appreciable numbers of neutrophils (Iacono *et al*, 2006). Levels of mRNA of the neutrophil chemoattractant CXCL2 were also quantified in this study. RJHM-infected brains had 1000-fold greater mRNA levels of CXCL2 when compared to the three other viruses (Figure 4 for RA59, and data not shown). Neutrophils may contribute to the very high virulence of RJHM. Antibody depletion of neutrophils, or inhibition of nitric oxide synthase during RJHM infection, resulted in reduced apoptosis and reduced brain destruction (Iacono et al, 2006). Mice infected with a more attenuated JHM and depleted of neutrophils demonstrated increased mortality and a concomitant loss in blood brain barrier integrity. (Zhou *et al*, 2003). Thus, the contribution of neutrophils to RJHM pathogenesis is strain dependent and warrants further study.

The kinetics of IFN-γ and IL-12 mRNA expression were examined. IFN-γ has been demonstrated to play a role in viral clearance of MHV (Lane *et al*, 1997; Parra *et al*, 1997; Pearce *et al*, 1994; Rempel *et al*, 2004a; Smith *et al*, 1991). In agreement with these previous reports, we found both IFN-γ and IL-12 were up-regulated after infection with RA59 and SJHM/RA59. This might be expected since both of

these viruses induce a robust CD8+ T-cell infiltration. We did not observe any differences in IL-10 protein or mRNA levels, nor in TGF-β mRNA, between any of the groups, suggesting the anti-inflammatory properties of these cytokines were not responsible for the lower amounts of IFN-γ and IL-12 produced during RJHM and SA59/RJHM infection (data not shown).

Although brain chemokine mRNA levels do not differ significantly during early infection with the different viruses, mRNA expression of all the chemokines and IFN-γ are elevated above mock by days 1 to 3, suggesting expression is from resident cells, not just infiltrating T cells. Although neurons can express CXCL10 and CCL2 (Flugel *et al*, 2001; Klein *et al*, 2005; Patterson *et al*, 2003), the majority of chemokines are produced by astrocytes and microglia (Hesselgesser and Horuk, 1999). Primary neurons infected with either RJHM or RA59 did not produce different levels of chemokine proteins (data not shown). However, astrocytes and microglia have been reported to produce CXCL10, CXCL9, and proinflammatory cytokine mRNAs, such as IL-12p40, during MHV infection (Lane *et al*, 1998; Li *et al*, 2004; Liu *et al*, 2001). Thus early infection of these different cell types may result in a different pattern of cytokines and chemokines that would influence the type of cellular infiltration. Indeed, when microglial or astrocyte cultures were infected with West Nile virus, different patterns of cytokine expression were reported (Cheeran *et al*, 2005). The tropism of RJHM and RA59 may therefore play a role in the initial chemokine/cytokine response.

Materials and methods

Viruses and inoculations

Chimeric (SJHM/RA59, SA59/RJHM) and wild-type recombinants (RA59, RJHM) were constructed and characterized as previously described (Navas and Weiss, 2003; Phillips *et al*, 1999, 2002). All experiments were performed using 4-week-old, male C57BL/6 mice (National Cancer Institute, Bethesda, MD). Mice were inoculated intracranially (i.c.) in the left cerebral hemisphere with 50 plaque forming units (PFU) of virus (diluted to a final volume of 20 μl in phosphate-buffered saline (PBS) with 0.75% bovine serum albumin) or diluent only for mock infection. Infections with wild-type recombinants (RA59, RJHM) and chimeric recombinants (SJHM/RA59, SA59/RJHM) were carried out at the same time and thus compared to the same mock-infected animals.

RNA extraction and quantification of relative viral genomes. At days 1, 3, 5, and 7 p.i., animals were euthanized and perfused via cardiac puncture with 10 ml of PBS. Each brain was divided sagittally and the right half of the brain was stored at -20°C in RNA Later (Ambion). RNA was isolated by homogenization in TRIzol (Invitrogen) followed by purification using the RNAeasy kit (Qiagen). RNA was quantified by spectroscopy and DNase treated twice using the DNA free kit (Ambion) to remove genomic DNA. To ensure that genomic DNA had been removed, quantitative polymerase chain reaction (PCR) on RNA samples was performed for 18S RNA without reverse transcriptase. Synthesis of cDNA was performed by first incubating 1 μg of total RNA with random hexamers for 3 min at 85°C. A mixture of first-strand buffer, dNTPs, RNase inhibitor (Amersham Biosciences), and Superscript II reverse transcriptase (Invitrogen) was then added to each sample and heated for 50 min at 42°C, followed by inactivation for 5 min at 95°C. To determine relative viral genome levels, real-time PCR was performed using 2 μl of cDNA generated as described above in a 25-μl reaction mixture containing iQ Sybrgreen master mix, water, and MHV primers (0.4 pmol) designed from a conserved region of the open reading frame (ORF) 1b sequence. Forward: 5′ ATGGCGTCTACATTAACACGAC 3′; reverse: 5′ TTACCTTGTGGGCTCCGGTA 3′. Real-time PCR was also performed for 18S RNA using the following primers: Forward: 5′ TTGTTGGTTTTCGGAACTGAGG 3′; reverse: 5′ GCAAATGCTTTCGCTCTGGTC 3′. MHV and 18S primers were designed on MacVector using sequences obtained from GenBank. Real-time PCR was performed using the iQ5 real-time PCR machine (BioRad). Each viral Ct was normalized to each sample's corresponding 18S Ct to obtain a ΔCt value ($Ct_{genome} - Ct_{18S}$). Average ΔCt and standard errors were calculated for each group. There is an inverse correlation between ΔCt and starting amounts of RNA, therefore the axes of the graphs are inverted to display this relationship. The ability to detect viral genomes in the brain also enabled us to determine the level of infection for each animal; occasionally an animal did not have detectable viral genomes, or had very low levels (<100-fold than other mice in the same group; data not shown). These animals were excluded from the chemokine analysis as their mRNA and protein chemokine levels were similar to those of mock-infected mice.

Quantitative real-time PCR for chemokine mRNA

Chemokine mRNA levels were quantified using custom-designed Low Density Array (LDA) cards (Applied Biosystems). Primers for cytokines included on the cards were CCL2, CCL3, CCL4, CCL5, CCL7, CXCL10, CXCL2, CXCL9, IFN-α, IFN-β, IFN-γ, IL-10, IL-12, IL-16, IL-1β, IL-2, IL-4, IL-5, IL-6, tumor necrosis factor (TNF)-α, and transforming growth factor (TGF)-β. LDA cards were run using the 7900 HT Sequence Detection System and analyzed with the SDS 2.1 software (Applied Biosystems). Cycle threshold (Ct) values generated for each cytokine target from each sample were normalized to 18S Ct values to give ΔCt values ($Ct_{target} - Ct_{18S}$). Average ΔCt values and standard errors were calculated for each

group. As described above, the axes of the graphs are inverted to display the inverse relationship between ΔCt values and the amount of starting RNA.

Protein preparation and analysis using multiplex bead arrays

To prepare protein for multiplex bead analysis, the left portion of the brains were harvested as described above, and flash frozen. Brains were then homogenized in PBS containing an EDTA-free protease inhibitor cocktail tablet (Complete Tabs; Roche). Homogenate were then centrifuged at $4000 \times g$ for 5 min at 4°C, and the supernatants collected for protein analysis. Protein concentration was determined using a standard Bradford assay (BioRad). Samples were diluted in PBS to 350 μg/ml and analyzed using a bead based protein multiplex assay platform (Luminex, Austin, TX) and a mouse Cytokine Twenty-Plex antibody bead kit (Invitrogen, Carlsbad, CA) according to manufacturer's instructions. Cytokines analyzed by the array include fibroblast growth factor (FGF), granulocyte-macrophage colony-stimulating factor (GM-CSF), IFN-γ, IL-1α, IL-1β, IL-2, IL-4, IL-5, IL-6, IL-10, IL-12, IL-13, IL-17, CXCL10, CXCL9, KC, CCL2, CCL3, TNF-α, and vascular endothelial growth factor (VEGF). Average concentrations and standard errors were calculated for each group.

Statistics

Statistical differences between groups were determined by one-way analysis of variance (ANOVA) with the Student-Newman-Kauls test for multiple comparisons using SigmaStat 3.1 software. P values of $<.05$ were considered significant.

References

Asensio VC, Campbell IL (2001). Chemokines and viral diseases of the central nervous system. *Adv Virus Res* **56:** 127–173.

Asensio VC, Maier J, Milner R, Boztug K, Kincaid C, Moulard M, Phillipson C, Lindsley K, Krucker T, Fox HS, Campbell IL (2001). Interferon-independent, human immunodeficiency virus type 1 gp120-mediated induction of CXCL10/IP-10 gene expression by astrocytes in vivo and in vitro. *J Virol* **75:** 7067–7077.

Bozic CR, Kolakowski LF Jr, Gerard NP, Garcia-Rodriguez C, von Uexkull-Guldenband C, Conklyn MJ, Breslow R, Showell HJ, Gerard C (1995). Expression and biologic characterization of the murine chemokine KC. *J Immunol* **154:** 6048–6057.

Center for Disease Control and Prevention (2006). West Nile virus: statistics, surveillance, and control. http://www.cdc.gov/ncidod/dvbid/westnile/surv&control.htm

Cheeran MC, Hu S, Sheng WS, Rashid A, Peterson PK (2005). Differential responses of human brain cells to West Nile virus infection. *J NeuroVirol* **11:** 512–524.

Collins AR, Knobler RL, Powell H, Buchmeier MJ (1982). Monoclonal antibodies to murine hepatitis virus-4 (strain JHM) define the viral glycoprotein responsible for attachment and cell–cell fusion. *Virology* **119:** 358–371.

Dalziel RG, Lampert PW, Talbot PJ, Buchmeier MJ (1986). Site-specific alteration of murine hepatitis virus type 4 peplomer glycoprotein E2 results in reduced neurovirulence. *J Virol* **59:** 463–471.

Dufour JH, Dziejman M, Liu MT, Leung JH, Lane TE, Luster AD (2002). IFN-gamma-inducible protein 10 (IP-10; CXCL10)-deficient mice reveal a role for IP-10 in effector T cell generation and trafficking. *J Immunol* **168:** 3195–3204.

Farber JM (1990). A macrophage mRNA selectively induced by {gamma}-interferon encodes a member of the platelet factor 4 family of cytokines. *Proc Natl Acad Sci USA* **87:** 5238–5242.

Farber JM (1997). Mig and IP-10: CXC chemokines that target lymphocytes. *J Leukoc Biol* **61:** 246–257.

Flugel A, Hager G, Horvat A, Spitzer C, Singer GMA, Graeber MB, Kreutzberg GW, Schwaiger F-W (2001). Neuronal MCP-1 Expression in Response to Remote Nerve Injury. *J Cereb Blood Flow Metab* **21:** 69–76.

Glass WG, Chen BP, Liu MT, Lane TE (2002). Mouse hepatitis virus infection of the central nervous system: chemokine-mediated regulation of host defense and disease. *Viral Immunol* **15:** 261–272.

Hesselgesser J, Horuk R (1999). Chemokine and chemokine receptor expression in the central nervous system. *J Neuro Virol* **5:** 13–26.

Iacono KT, Kazi L, Weiss SR (2006). Both spike and background genes contribute to murine coronavirus neurovirulence. *J Virol* **80:** 6834–6843.

Klein RS, Lin E, Zhang B, Luster AD, Tollett J, Samuel MA, Engle M, Diamond MS (2005). Neuronal CXCL10 directs CD8+ T-cell recruitment and control of West Nile virus encephalitis. *J Virol* **79:** 11457–11466.

Lane TE, Asensio VC, Yu N, Paoletti AD, Campbell IL, Buchmeier MJ (1998). Dynamic regulation of alpha- and beta-chemokine expression in the central nervous system during mouse hepatitis virus-induced demyelinating disease. *J Immunol* **160:** 970–978.

Lane TE, Liu MT, Chen BP, Asensio VC, Samawi RM, Paoletti AD, Campbell IL, Kunkel SL, Fox HS, Buchmeier MJ (2000). A central role for CD4+ T Cells and RANTES in virus-induced central nervous system inflammation and demyelination. *J Virol* **74:** 1415–1424.

Lane TE, Paoletti AD, Buchmeier MJ (1997). Disassociation between the In vitro and in vivo effects of nitric oxide on a neurotropic murine coronavirus. *J Virol* **71:** 2202–2210.

Lavi E, Gilden DH, Highkin MK, Weiss SR (1984a). Persistence of mouse hepatitis virus A59 RNA in a slow virus demyelinating infection in mice as detected by in situ hybridization. *J Virol* **51:** 563–566.

Lavi E, Gilden DH, Wroblewska Z, Rorke SB, Weiss SR (1984b). Experimental demyelination produced by the A59 strain of mouse hepatitis virus. *Neurology* **34:** 597–603.

Li Y, Fu L, Gonzales DM, Lavi E (2004). Coronavirus neurovirulence correlates with the ability of the virus to induce proinflammatory cytokine signals from astrocytes and microglia. *J Virol* **78:** 3398–406.

Liu MT, Armstrong D, Hamilton TA, Lane TE (2001). Expression of Mig (monokine induced by interferon-gamma) is important in T lymphocyte recruitment and host defense following viral infection of the central nervous system. *J Immunol* **166:** 1790–1795.

Liu MT, Chen BP, Oertel P, Buchmeier MJ, Armstrong D, Hamilton TA, Lane TE (2000). The T cell chemoattractant IFN-inducible protein 10 is essential in host defense against viral-induced neurologic disease. *J Immunol* **165:** 2327–2330.

Loetscher P, Seitz M, Clark-Lewis I, Baggiolini M, Moser B (1994). Monocyte chemotactic proteins MCP-1, MCP-2, and MCP-3 are major attractants for human CD4+ and CD8+ T lymphocytes. *FASEB J* **8:** 1055–1060.

Luster AD, Ravetch JV (1987). Biochemical characterization of a gamma interferon-inducible cytokine (IP-10). *J Exp Med* **166:** 1084–1097.

MacNamara KC, Chua MM, Nelson PT, Shen H, Weiss SR (2005). Increased epitope-specific CD8+ T cells prevent murine coronavirus spread to the spinal cord and subsequent demyelination. *J Virol* **79:** 3370–3381.

Manchester M, Eto DS, Oldstone MB (1999). Characterization of the inflammatory response during acute measles encephalitis in NSE-CD46 transgenic mice. *J Neuroimmunol* **96:** 207–217.

Marques CP, Hu S, Sheng W, Lokensgard JR (2006). Microglial cells initiate vigorous yet non-protective immune responses during HSV-1 brain infection. *Virus Res* **121:** 1–10.

Matsushima K, Larsen CG, DuBois GC, Oppenheim JJ (1989). Purification and characterization of a novel monocyte chemotactic and activating factor produced by a human myelomonocytic cell line. *J Exp Med* **169:** 1485–90.

Navas S, Seo SH, Chua MM, Sarma JD, Lavi E, Hingley ST, Weiss SR (2001). Murine coronavirus spike protein determines the ability of the virus to replicate in the liver and cause hepatitis. *J Virol* **75:** 2452–7.

Navas S, Weiss SR (2003). Murine coronavirus-induced hepatitis: JHM genetic background eliminates A59 spike-determined hepatotropism. *J Virol* **77:** 4972–4978.

Parra B, Hinton DR, Lin MT, Cua DJ, Stohlman SA (1997). Kinetics of cytokine mRNA expression in the central nervous system following lethal and nonlethal coronavirus-induced acute encephalomyelitis. *Virology* **233:** 260–70.

Patterson CE, Daley JK, Echols LA, Lane TE, Rall GF (2003). Measles virus infection induces chemokine synthesis by neurons. *J Immunol* **171:** 3102–3109.

Pearce BD, Hobbs MV, McGraw TS, Buchmeier MJ (1994). Cytokine induction during T-cell-mediated clearance of mouse hepatitis virus from neurons in vivo. *J Virol* **68:** 5483–95.

Phillips JJ, Chua MM, Lavi E, Weiss SR (1999). Pathogenesis of chimeric MHV4/MHV-A59 recombinant viruses: the murine coronavirus spike protein is a major determinant of neurovirulence. *J Virol* **73:** 7752–7760.

Phillips JJ, Chua MM, Rall GF, Weiss SR (2002). Murine coronavirus spike glycoprotein mediates degree of viral spread, inflammation, and virus-immunpathology in the central nervous system. *Virology* **301:** 109–120.

Ransohoff RM, Wei T, Pavelko KD, Lee JC, Murray PD, Rodriguez M (2002). Chemokine expression in the central nervous system of mice with a viral disease resembling multiple sclerosis: roles of CD4+ and CD8+ T cells and viral persistence. *J Virol* **76:** 2217–24.

Rempel JD, Murray SJ, Meisner J, Buchmeier MJ (2004a). Differential regulation of innate and adaptive immune responses in viral encephalitis. *Virology* **318:** 381–392.

Rempel JD, Murray SJ, Meisner J, Buchmeier MJ (2004b). Mouse hepatitis virus neurovirulence: evidence of a linkage between S glycoprotein expression and immunopathology. *Virology* **318:** 45–54.

Rubio N, Sanz-Rodriguez F, Lipton HL (2006). Theiler's virus induces the MIP-2 chemokine (CXCL2) in astrocytes from genetically susceptible but not from resistant mouse strains. *Cell Immunol* **239:** 31–40.

Sanders VJ, Pittman CA, White MG, Wang G, Wiley CA, Achim CL (1998). Chemokines and receptors in HIV encephalitis. *AIDS* **12:** 1021–1026.

Sellner J, Dvorak F, Zhou Y, Haas J, Kehm R, Wildemann B, Meyding-Lamade U (2005). Acute and long-term alteration of chemokine mRNA expression after anti-viral and anti-inflammatory treatment in herpes simplex virus encephalitis. *Neurosci Lett* **374:** 197–202.

Shirato K, Kimura T, Mizutani T, Kariwa H, Takashima I (2004). Different chemokine expression in lethal and non-lethal murine West Nile virus infection. *J Med Virol* **74:** 507–13.

Smith AL, Barthold SW, de Souza MS, Bottomly K (1991). The role of gamma interferon in infection of susceptible mice with murine coronavirus, MHV-JHM. *Arch Virol* **121:** 89–100.

Standiford TJ, Rolfe MW, Kunkel SL, Lynch JPd, Burdick MD, Gilbert AR, Orringer MB, Whyte RI, Strieter RM (1993). Macrophage inflammatory protein-1 alpha expression in interstitial lung disease. *J Immunol* **151:** 2852–2863.

Stiles LN, Hardison JL, Schaumburg CS, Whitman LM, Lane TE (2006a). T cell antiviral effector function is not dependent on CXCL10 following murine coronavirus infection. *J Immunol* **177:** 8372–8380.

Stiles LN, Hosking MP, Edwards RA, Strieter RM, Lane TE (2006b). Differential roles for CXCR3 in CD4+ and CD8+ T cell trafficking following viral infection of the CNS. *Eur J Immunol* **36:** 613–622.

van Gassen KLI, Netzeband JG, de Graan PNE, Gruol DL (2005). The chemokine CCL2 modulated Ca2+ dynamics and electrophysiological properties of cultured cerebellar Purkinje neurons. *Eur J Neurosci* **21:** 2949–57.

Wang JM, Sherry B, Fivash MJ, Kelvin DJ, Oppenheim JJ (1993). Human recombinant macrophage inflammatory protein-1 alpha and -beta and monocyte chemotactic and activating factor utilize common and unique receptors on human monocytes. *J Immunol* **150:** 3022–29.

Williamson JSP, Stohlman SA (1990). Effective clearance of mouse hepatitis virus from the central nervous system requires both CD4+ and CD8+ T cells. *J Virol* **64:** 4589–92.

Winter PM, Dung NM, Loan HT, Kneen R, Wills B, Thu LT, House D, White NJ, Farrar JJ, Hart CA, Solomon T (2004). Proinflammatory cytokines and chemokines in humans with Japanese encephalitis. *J Infect Dis* **190:** 1618–26.

Wolpe SD, Sherry B, Juers D, Davatelis G, Yurt RW, Cerami A (1989). Identification and characterization of macrophage inflammatory protein 2. *Proc Natl Acad Sci USA* **86:** 612–616.

World Health Organization (2005). Outbreak encephalitis 2005: cases of Japanese encephalitis in Gorakhpur, Uttar Pradesh, India. In: *Core programme clusters communicable diseases and disease surveillance*. http://w3.whosea.org/en/Section1226/Section2073.asp

Xu J, Zhong S, Liu J, Li L, Li Y, Wu X, Li Z, Deng P, Zhang J, Zhong N, Ding Y, Jiang Y (2005). Detection of severe acute respiratory syndrome coronavirus in the brain: potential role of the chemokine mig in pathogenesis. *Clin Infect Dis* **41:** 1089–96.

Zhou J, Stohlman SA, Hinton DR, Marten NW (2003). Neutrophils promote mononuclear cell infiltration during viral-induced encephalitis. *J Immunol* **170:** 3331–3336.